

Thermal atomic layer etching of crystalline GaN using sequential exposures of XeF₂ and BCl₃

Cite as: Appl. Phys. Lett. **114**, 243103 (2019); doi: [10.1063/1.5095938](https://doi.org/10.1063/1.5095938)

Submitted: 13 March 2019 · Accepted: 27 May 2019 ·

Published Online: 17 June 2019 · Publisher error corrected 21 June 2019



View Online



Export Citation



CrossMark

Nicholas R. Johnson,¹ Jennifer K. Hite,² Michael A. Mastro,²  Charles. R. Eddy, Jr.,² and Steven M. George^{1,a)} 

AFFILIATIONS

¹Department of Chemistry, University of Colorado, Boulder, Colorado 80309, USA

²U.S. Naval Research Laboratory (NRL), Washington, D.C. 20375, USA

^{a)}Electronic mail: Steven.George@Colorado.edu

ABSTRACT

Gallium nitride (GaN) is a wide-bandgap semiconductor that is useful for optoelectronics and high speed and high power electronics. Fabrication of GaN devices requires etching for many processing steps. Gas phase thermal atomic-layer-controlled etching is desirable for damage-free isotropic etching. In this letter, the thermal atomic layer etching (ALE) of crystalline GaN was demonstrated using sequential exposures of XeF₂ and BCl₃. GaN ALE was achieved with an etch rate of 0.55 Å/cycle at 195 °C using XeF₂ exposures for 20 s at 40 mTorr and BCl₃ exposures for 0.5 s at 50 mTorr. At the same reactant exposures, GaN etch rates varied with temperature from 0.18 Å/cycle at 170 °C to 0.72 Å/cycle at 300 °C. The GaN etch rates increased slowly with increasing XeF₂ exposure. In addition, the GaN etch rate was self-limiting with respect to both increasing BCl₃ pressures and BCl₃ exposure times. This self-limiting behavior for BCl₃ is consistent with a ligand-exchange mechanism for GaN ALE. Alternative fluorination reactants were also investigated including HF, SF₄, and NF₃ plasma. Sequential exposures of NF₃ plasma and BCl₃ yielded GaN etch rates of 2.5–2.9 Å/cycle at 250 °C. In contrast, the HF and SF₄ fluorination reactants could not etch crystalline GaN.

Published under license by AIP Publishing. <https://doi.org/10.1063/1.5095938>

Atomic layer etching (ALE) is based upon sequential, self-limiting reactions that can remove material with control at the atomic scale.¹ ALE can be achieved using both plasma and thermal processes.^{1,2} ALE proceeds via two steps: surface modification followed by the removal of the modified surface. For plasma ALE, a halogen or halocarbon film is adsorbed onto the surface.¹ After adsorption, ions impact the surface and lead to the etching of the modified surface layer. Plasma ALE has been used to etch a variety of materials including Si,^{3,4} SiO₂,⁵ Al₂O₃,⁶ HfO₂,⁷ and InP.⁸ Plasma ALE is useful for anisotropic etching.

Thermal ALE has also been developed recently using a number of pathways. Thermal ALE is the reverse of thermal atomic layer deposition (ALD).^{9,10} The first demonstration of thermal ALE utilized fluorination for surface modification.² The fluoride layer was then removed by a ligand-exchange reaction. Other mechanisms involve the conversion of the surface layer to a new material.^{11–13} This new material then becomes volatile by fluorination and ligand-exchange or fluorination to a volatile fluoride. Thermal ALE has been demonstrated for a number of materials including amorphous Al₂O₃,^{2,14} HfO₂,¹⁵ and SiO₂,¹² and crystalline Si,¹⁶ ZnO,¹¹ W,¹³ and AlN.¹⁷ Thermal ALE is useful for isotropic etching.

GaN is an important direct-bandgap semiconductor used to fabricate light-emitting diodes and laser diodes.^{18,19} In addition to its optoelectronic properties, GaN has a high thermal stability and large piezoelectric constant and is chemically inert. GaN is very useful for high temperature and high power electronics based on high electron mobility transistors (HEMTs).^{20–22} GaN nanowire transistor devices have also exhibited high electron mobilities.^{23,24}

Dry plasma etching techniques are useful for fabricating GaN devices.²⁵ Plasma etching of GaN uses primarily chlorine-containing plasmas to produce volatile GaCl₃.²⁵ Various chlorine-containing plasmas are formed using Cl₂ and BCl₃.^{26,27} GaN can also be etched by low energy electron enhanced etching in H₂ plasmas.²⁸ There is no wet-etch chemistry for etching crystalline GaN prepared using metal organic chemical vapor deposition (MOCVD) techniques.²⁹

Plasma GaN ALE has recently been demonstrated by chlorination of the GaN surface followed by ion bombardment to remove GaCl_x species.^{30,31} Plasma GaN ALE will be useful for directional and anisotropic GaN ALE. In contrast, there are no reported thermal approaches for isotropic GaN ALE. Isotropic thermal GaN ALE should be useful for the fabrication of GaN devices including light emitting diodes and high electron mobility transistors. Thermal GaN

ALE should also be valuable for fabricating nanoscale and nanowire GaN devices that are difficult to etch without damage.

The crystalline GaN sample used in this study was grown in a Thomas Swan metal organic chemical vapor deposition (MOCVD) vertical showerhead reactor. The sample consisted of a 2 in. a-plane sapphire substrate with a 25 nm thick AlN nucleation layer and a 300 nm thick unintentionally doped epitaxial GaN layer. The GaN was grown using trimethylgallium and ammonia using the following conditions: growth temperature of 1025 °C, V/III ratio of 2000, and pressure of 60 Torr.³²

The GaN sample was cut into 1/2 in. square coupons and cleaned in a hot (85 °C) HCl bath to remove the native oxide. Subsequently, the coupons were sonicated for 10 min in acetone, ethanol, and lastly isopropanol. The coupons were then heated on a stage in a reactor that has been described previously.³³ Prior to coupon introduction, the reactor walls were coated with 1500 cycles of Al₂O₃ ALD using trimethylaluminum [TMA, Al(CH₃)₃] and H₂O followed by 100 cycles of AlF₃ ALD with Al(CH₃)₃ and HF. These coatings passivated the reactor walls and ensured that the etching reactants did not interact with stainless steel surfaces. The reactor walls were heated to 170 °C.

The crystalline GaN films were analyzed by *in situ* spectroscopic ellipsometry (SE) using an M-2000D ellipsometer from J. A. Woollam. The incident angle for all SE experiments was 70°. The spectral range was 239.2–1687.2 nm. GaN film thicknesses were measured after each full reaction cycle or after each XeF₂ or BCl₃ reaction. Changes in the GaN film thickness were analyzed using the Complete Ease software from J. A. Woollam. A model consisting of a P_{Semi}-MO, two P_{Semi}-Tri, and a Gaussian oscillator was used for the thickness determination.

Boron trichloride (99.9%, Synquest Laboratories), xenon difluoride (99.5%, Strem Chemicals), HF-pyridine (70 wt. % HF Sigma-Aldrich), SF₄ (94% Synquest Laboratories), and NF₃ (99.9% Airgas) were used as the reactants. Reactants were dosed separately into the reactor under a stream of argon. In other experiments, the reactants were held statically in the reactor for a defined amount of time. The reactants were introduced using two pneumatic valves on either side of a conductance-limiting valve.

Between reactant doses, a stream of argon at a pressure of 1270 mTorr was used to flush out excess reactant. A purge time of 60 s was used between repeated XeF₂ exposures. SF₄, NF₃, and BCl₃ purge times were 60 s regardless of viscous or static dosing. HF purge times were slightly larger at 70 s because of the longer HF residence time. The chamber was pumped by a dual stage rotary mechanical pump (Alcatel Adixen Pascal 2015 SD pump).

Fluorine radicals for GaN fluorination were produced by an inductively coupled plasma (ICP) generated from NF₃ gas. The ICP source was a quartz tube (6 cm inner diameter × 25 cm long) residing inside a helical copper coil. A 50 Ω impedance matching network (Navigator Digital Matching Network, Advanced Energy) was used in conjunction with a 13.56 MHz RF generator (Paramount RF Power Supply, Advanced Energy) to ignite the ICP plasma. The distance between the ICP source and the GaN substrate was ~4 cm.

This work investigates the ALE of crystalline GaN using XeF₂ and BCl₃ as the reactants. These reactants could lead to etching by two different pathways. XeF₂ could initially fluorinate the surface of GaN by the reaction GaN(s) + 3XeF₂(g) → GaF₃(s) + NF₃(g) + 3Xe(g). This reaction is spontaneous with a standard free energy change of

$\Delta G^\circ = -216 \text{ kcal/mol}$ at 200 °C.³⁴ GaF₃ is stable in vacuum until 550 °C.³⁵ The GaF₃ surface layer could then undergo a ligand-exchange with BCl₃ by the reaction GaF₃(s) + BCl₃(g) → GaCl₃(g) + BF₃(g). This reaction is spontaneous with $\Delta G^\circ = -19 \text{ kcal/mol}$ at 200 °C.³⁴

Alternatively, BCl₃ could initially convert GaN to BN by the reaction GaN(g) + BCl₃(g) → BN(s) + GaCl₃(g). This conversion reaction is spontaneous with $\Delta G^\circ = -43 \text{ kcal/mol}$ at 200 °C.³⁴ The BN surface layer could then be etched by XeF₂ by the reaction BN(s) + 3XeF₂(g) → BF₃(g) + NF₃(g) + 3Xe(g). This reaction is spontaneous with $\Delta G^\circ = -192 \text{ kcal/mol}$ at 200 °C.³⁴ The actual etching pathway could be either fluorination and ligand-exchange or conversion and fluorination to a volatile fluoride.

Figure 1 shows the GaN thickness vs number of reaction cycles measured by *in situ* SE. Each reaction cycle was the sequential exposure of XeF₂ first and then BCl₃. The XeF₂ exposure was conducted statically for 20 s at 40 mTorr. The BCl₃ exposure was performed for 0.5 s at 50 mTorr under viscous flow conditions. Between each reactant exposure, the chamber was purged by argon gas for 60 s. Figure 1 displays the change of the GaN thickness over 30 cycles at 195 °C. Each data point represents a thickness measurement after one complete reaction cycle.

The etch rate for the GaN ALE results in Fig. 1 at 195 °C is 0.55 Å/cycle. The GaN etching is linear with an R² value of 0.999. Multiple GaN ALE experiments were performed at 195 °C under the same conditions. The GaN etch rate varied slightly from 0.50 to 0.59 Å/cycle. This GaN etch rate is much less than the etch rate of ~4 Å/cycle obtained with plasma GaN ALE using plasma chlorination or Cl₂ adsorption and Ar ion exposures.^{30,31} The GaN etch rate of 0.55 Å/cycle is also much less than the crystalline GaN lattice constants of a = 3.18 Å and c = 5.18 Å.³⁶ Both XeF₂ and BCl₃ were required for GaN etching. No changes in GaN thickness or optical properties were observed for repeated BCl₃ exposures. Likewise, XeF₂ alone did not etch GaN.

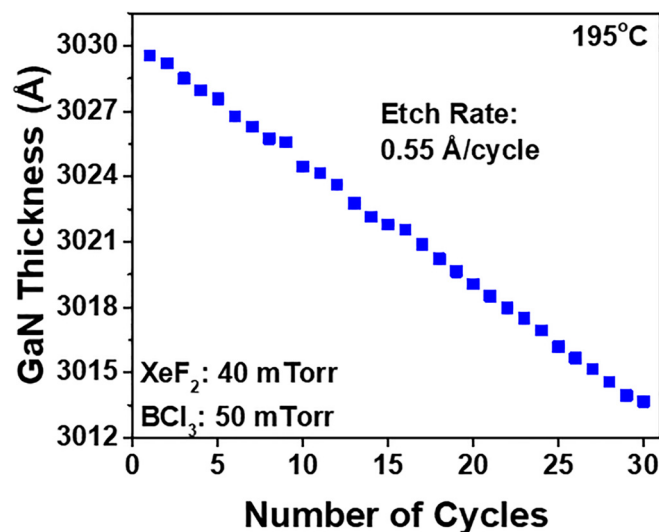


FIG. 1. GaN film thickness vs number of sequential XeF₂ and BCl₃ exposures at 195 °C. The GaN etch rate is 0.55 Å/cycle.

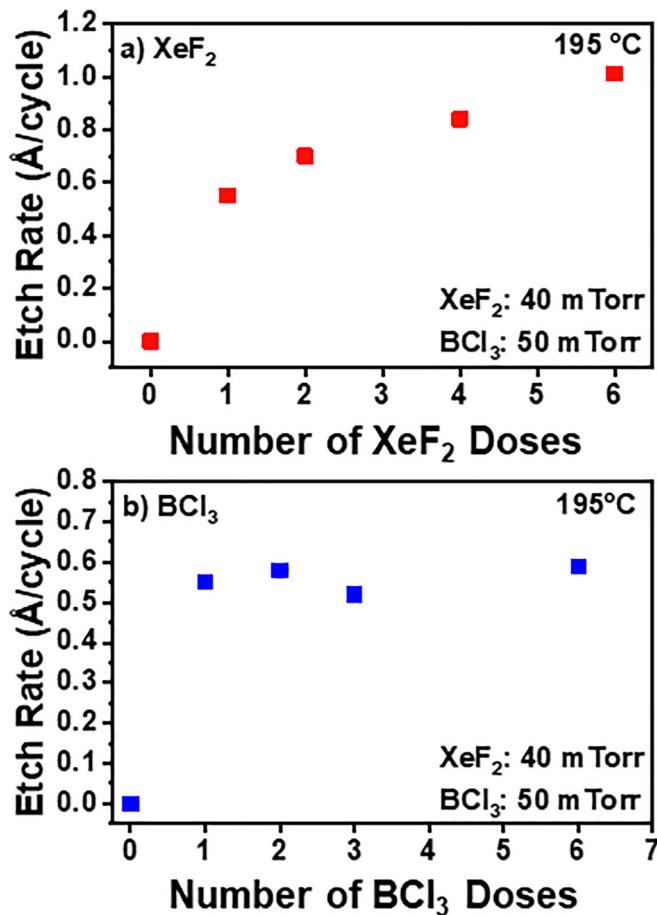


FIG. 2. (a) GaN etch rate at 195 °C vs number of XeF₂ doses with a fixed BCl₃ exposure and (b) GaN etch rate at 195 °C vs number of BCl₃ doses with a fixed XeF₂ exposure.

Figure 2 examines the self-limiting reactions of XeF₂ and BCl₃ during GaN ALE at 195 °C. In Fig. 2(a), the BCl₃ exposure was constant at 50 mTorr for 0.5 s while varying the number of XeF₂ doses. Each XeF₂ dose was a static XeF₂ exposure for 20 s at 40 mTorr. The GaN etch rate begins to slow its rate of increase with a larger number of XeF₂ doses. The etch rate reaches an etch rate of 1.0 Å/cycle after 6 XeF₂ doses. The slight increase in the GaN etch rate for larger XeF₂ exposures will affect the conformality of GaN ALE in high aspect ratio structures.

XeF₂ fluorinates GaN and is believed to form GaF₃ on the surface by the reaction $\text{GaN(s)} + 3\text{XeF}_2(\text{g}) \rightarrow \text{GaF}_3(\text{s}) + \text{NF}_3(\text{g}) + 3\text{Xe}(\text{g})$. However, the thickness of the GaF₃ layer is below the detection limit of SE. No change in ψ and Δ was observed after XeF₂ exposures at 195 °C. Even 60 repeated XeF₂ exposures at 40 mTorr for 20 s did not result in any observable change in ψ and Δ .

In Fig. 2(b), the XeF₂ exposure was conducted statically for 20 s at 40 mTorr while varying the number of BCl₃ doses. Each BCl₃ dose was a BCl₃ exposure for 0.5 s at 50 mTorr under viscous flow conditions. The GaN etch rate quickly saturates at an etch rate of 0.55 Å/cycle. The lack of BCl₃ exposure dependence argues for a ligand-

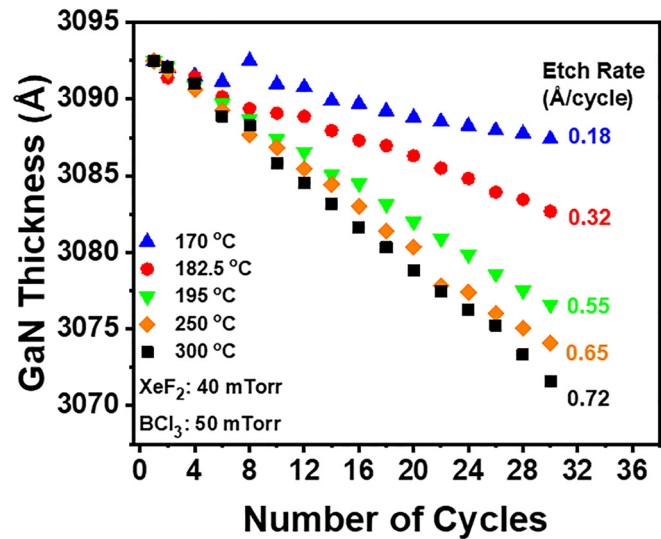


FIG. 3. GaN film thickness vs number of sequential XeF₂ and BCl₃ exposures at various temperatures.

exchange mechanism for GaN ALE. The ligand-exchange reaction is hypothesized to be $\text{GaF}_3(\text{s}) + \text{BCl}_3(\text{g}) \rightarrow \text{GaCl}_3(\text{g}) + \text{BF}_3(\text{g})$ or $\text{GaF}_3(\text{s}) + 3\text{BCl}_3(\text{g}) \rightarrow \text{GaCl}_3(\text{g}) + 3\text{BFCl}_2(\text{g})$ if each BCl₃ reactant participates in only one ligand-exchange reaction.

If the GaN ALE was occurring by a conversion mechanism,^{11,12} then the etch rate should have increased with BCl₃ exposure. Other conversion mechanisms for ALE have observed larger etch rates with higher reactant exposures and pressures.^{11,12} The conversion layer acts as a diffusion barrier that slows the conversion reaction. However, higher exposures and higher pressures lead to more diffusion, higher conversion, and larger etching rates.

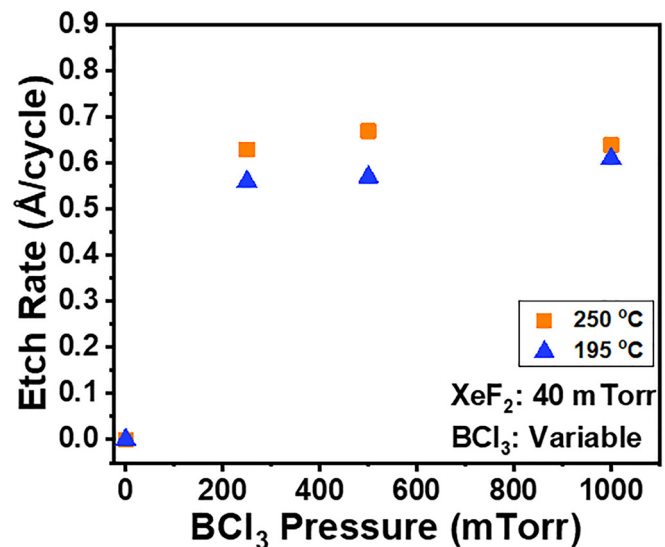


FIG. 4. GaN etch rate vs BCl₃ pressure during the BCl₃ exposure at 195 and 250 °C.

The change in GaN thickness vs number of cycles at varying temperatures is displayed in Fig. 3. The XeF₂ exposure was conducted statically for 20 s at 40 mTorr. The BCl₃ exposure was performed for 0.5 s at 50 mTorr under viscous flow conditions. All thicknesses were referenced to the same initial thickness of 3093 Å to show variations in etching at 170, 182.5, 195, 250, and 300 °C. The GaN etching is linear at all temperatures over the 30 reaction cycles. For the temperatures of 170, 182.5, 195, 250, and 300 °C, the etch rates were 0.18, 0.32, 0.55, 0.65, and 0.72 Å/cycle, respectively. The increase in the etch rate with temperature is attributed to a thicker fluoride surface layer formed by XeF₂ at higher temperatures. This fluoride layer is then removed by the ligand-exchange reaction with BCl₃.

To confirm that the BCl₃ reaction is not converting GaN to BN via the reaction $\text{GaN(s)} + \text{BCl}_3\text{(g)} \rightarrow \text{BN(s)} + \text{GaCl}_3\text{(g)}$, the GaN etch rate was examined vs BCl₃ pressure at both 195 and 250 °C. If BCl₃ converts GaN to BN, then the etch rate should increase with BCl₃ pressure. This increase would result from the larger amount of GaN conversion to BN at higher BCl₃ pressures. Similar behavior is observed during silicon oxidation where the SiO₂ layer on the silicon substrate acts as a diffusion barrier to further oxidation. This self-limiting oxidation is described by Deal–Grove kinetics.^{37,38} Higher O₂ or H₂O pressures facilitate oxygen diffusion through the SiO₂ layer on the silicon substrate.

Figure 4 reveals that the GaN etch rate does not increase vs BCl₃ pressure. The BCl₃ pressures of 250, 500, and 1000 mTorr were held statically for 5 s. The XeF₂ pressure was maintained at 40 mTorr for 20 s. At 195 °C, the GaN etch rates were 0.56, 0.57, and 0.62 Å/cycle at BCl₃ pressures of 250, 500, and 1000 mTorr, respectively. At 250 °C, the GaN etch rates were 0.63, 0.68, and 0.63 Å/cycle at BCl₃ pressures of 250, 500, and 1000 mTorr, respectively. These constant GaN etch rates argue against a conversion mechanism and support a ligand-exchange reaction. Mass spectrometry studies of the reaction products of the XeF₂ and BCl₃ reactions are needed to confirm the proposed ligand-exchange mechanism.

Additional experiments explored HF and SF₄ as fluorination reactants for GaN ALE. HF or SF₄ doses were held statically for 20 s at pressures of 300 or 500 mTorr. BCl₃ exposures were performed at 50 mTorr for 0.5 s. Under these reaction conditions, there was no evidence of GaN etching over 20 reaction cycles. The lack of GaN etching is attributed to the resistance of the crystalline GaN to these fluorination sources. Crystalline GaN has been previously shown to be chemically resistant to a variety of hot acids.²⁹ HF and SF₄ are thermodynamically predicted to fluorinate GaN to GaF₃. However, the values of $\Delta G^\circ = -37$ and -114 kcal/mol for fluorination at 250 °C by HF and SF₄, respectively, are lower than $\Delta G^\circ = -217$ kcal/mol for fluorination at 250 °C by XeF₂.³⁴

Fluorine radicals from a NF₃ plasma were also used to fluorinate GaN. Figure 5 displays the GaN thickness vs number of reaction cycles at 250 °C. NF₃ was dosed into the chamber at a pressure of 40 mTorr for 25 s. The plasma was formed after 5 s at a power of 75 W for the remaining 20 s. After the NF₃ plasma exposure, BCl₃ was dosed into the chamber for 0.5 s at a pressure of 50 mTorr. Figure 5 shows that the GaN etch rate is 2.85 Å/cycle over the 20 cycles. Individual experiments using NF₃ plasma exposures measured GaN etch rates varying from 2.5–2.9 Å/cycle. These GaN etch rates are much higher than the etch rate of 0.65 Å/cycle at 250 °C obtained using XeF₂ and BCl₃ in Fig. 3. The higher GaN etch rates are attributed to the thicker fluoride layers formed by the fluorine radicals.

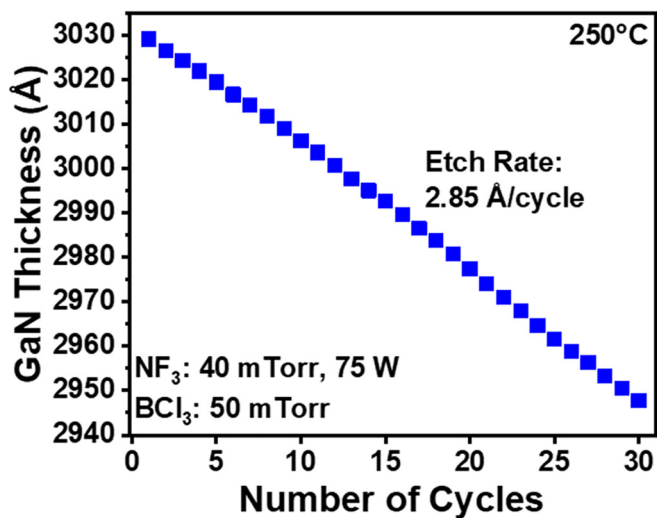


FIG. 5. GaN film thickness vs number of sequential NF₃ plasma and BCl₃ exposures at 250 °C. The GaN etch rate is 2.85 Å/cycle.

In summary, the thermal ALE of crystalline GaN was demonstrated using XeF₂ and BCl₃ as the reactants. The GaN etch rates were dependent on temperature and ranged from 0.18 Å/cycle at 170 °C to 0.72 Å/cycle at 300 °C. The GaN etch rates were reasonably self-limiting with XeF₂ exposure at 195 °C and the fluoride thickness on GaN after XeF₂ exposure was below the SE detection limit. The GaN etch rates were also self-limiting vs BCl₃ pressure and exposure. This behavior argued for a ligand-exchange mechanism for BCl₃. Strong fluorination reactants, such as fluorine radicals from the NF₃ plasma, produced higher GaN etch rates of 2.85 Å/cycle at 250 °C. In contrast, weaker nucleophilic fluorination reactants, such as HF and SF₄, were not able to etch crystalline GaN. Many uses for thermal GaN ALE are possible including etching recessed gates in GaN/AlGaN HEMTs and diameter reduction and surface smoothening of GaN nanowires.

The research conducted at the University of Colorado was funded by the Semiconductor Research Corporation (SRC). The research conducted at the U.S. Naval Research Laboratory was supported by the Office of Naval Research. The authors thank Advanced Energy for equipment used for the inductively coupled plasma (ICP) source.

REFERENCES

- ¹K. J. Kanarik, T. Lill, E. A. Hudson, S. Sriraman, S. Tan, J. Marks, V. Vahedi, and R. A. Gottscho, *J. Vac. Sci. Technol. A* **33**, 020802 (2015).
- ²Y. Lee and S. M. George, *ACS Nano* **9**, 2061–2070 (2015).
- ³S. D. Park, D. H. Lee, and G. Y. Yeom, *Electrochem. Solid State Lett.* **8**, C106–C109 (2005).
- ⁴H. Sakaue, S. Iseda, K. Asami, J. Yamamoto, M. Hirose, and Y. Horiike, *Jpn. J. Appl. Phys., Part 1* **29**, 2648–2652 (1990).
- ⁵D. Metzler, R. L. Bruce, S. Engelmann, E. A. Joseph, and G. S. Oehrlein, *J. Vac. Sci. Technol. A* **32**, 020603 (2014).
- ⁶K. S. Min, S. H. Kang, J. K. Kim, Y. I. Jhon, M. S. Jhon, and G. Y. Yeom, *Microelectron. Eng.* **110**, 457–460 (2013).
- ⁷J. B. Park, W. S. Lim, B. J. Park, I. H. Park, Y. W. Kim, and G. Y. Yeom, *J. Phys. D: Appl. Phys.* **42**, 055202 (2009).

- ⁸S. D. Park, C. K. Oh, J. W. Bae, G. Y. Yeom, T. W. Kim, J. I. Song, and J. H. Jang, *Appl. Phys. Lett.* **89**, 043109 (2006).
- ⁹T. Faraz, F. Roozeboom, H. C. M. Knoops, and W. M. M. Kessels, *ECS J. Solid State Sci. Technol.* **4**, N5023–N5032 (2015).
- ¹⁰S. M. George, *Chem. Rev.* **110**, 111–131 (2010).
- ¹¹D. R. Zywotko and S. M. George, *Chem. Mater.* **29**, 1183–1191 (2017).
- ¹²J. W. DuMont, A. E. Marquardt, A. M. Cano, and S. M. George, *ACS Appl. Mater. Interfaces* **9**, 10296–10307 (2017).
- ¹³N. R. Johnson and S. M. George, *ACS Appl. Mater. Interfaces* **9**, 34435–34447 (2017).
- ¹⁴Y. Lee, J. W. DuMont, and S. M. George, *Chem. Mater.* **28**, 2994–3003 (2016).
- ¹⁵Y. Lee and S. M. George, *J. Vac. Sci. Technol. A* **36**, 061504 (2018).
- ¹⁶A. I. Abdulagatov and S. M. George, *Chem. Mater.* **30**, 8465–8475 (2018).
- ¹⁷N. R. Johnson, H. X. Sun, K. Sharma, and S. M. George, *J. Vac. Sci. Technol. A* **34**, 050603 (2016).
- ¹⁸S. P. DenBaars, D. Feezell, K. Kelchner, S. Pimputkar, C. C. Pan, C. C. Yen, S. Tanaka, Y. J. Zhao, N. Pfaff, R. Farrell, M. Iza, S. Keller, U. Mishra, J. S. Speck, and S. Nakamura, *Acta Mater.* **61**, 945–951 (2013).
- ¹⁹S. Nakamura and M. R. Krames, *Proc. IEEE* **101**, 2211–2220 (2013).
- ²⁰K. J. Chen, O. Haberlen, A. Lidow, C. L. Tsai, T. Ueda, Y. Uemoto, and Y. F. Wu, *IEEE Trans. Electron Devices* **64**, 779–795 (2017).
- ²¹U. K. Mishra, L. Shen, T. E. Kazior, and Y. F. Wu, *Proc. IEEE* **96**, 287–305 (2008).
- ²²E. A. Jones, F. Wang, and D. Costinett, *IEEE J. Emerging Sel. Top. Power Electron.* **4**, 707–719 (2016).
- ²³Y. Huang, X. F. Duan, Y. Cui, and C. M. Lieber, *Nano Lett.* **2**, 101–104 (2002).
- ²⁴A. Motayed, M. Vaudin, A. V. Davydov, J. Melngailis, M. Q. He, and S. N. Mohammad, *Appl. Phys. Lett.* **90**, 043104 (2007).
- ²⁵S. J. Pearton, J. C. Zolper, R. J. Shul, and F. Ren, *J. Appl. Phys.* **86**, 1–78 (1999).
- ²⁶M. E. Lin, Z. F. Fan, Z. Ma, L. H. Allen, and H. Morkoc, *Appl. Phys. Lett.* **64**, 887–888 (1994).
- ²⁷R. J. Shul, G. B. McClellan, S. A. Casalnuovo, D. J. Rieger, S. J. Pearton, C. Constantine, C. Barratt, R. F. Karlicek, C. Tran, and M. Schurman, *Appl. Phys. Lett.* **69**, 1119–1121 (1996).
- ²⁸H. P. Gillis, D. A. Choutov, K. P. Martin, S. J. Pearton, and C. R. Abernathy, *J. Electrochem. Soc.* **143**, L251–L253 (1996).
- ²⁹D. Zhuang and J. H. Edgar, *Mater. Sci. Eng. R: Rep.* **48**, 1–46 (2005).
- ³⁰C. Kauppinen, S. A. Khan, J. Sundqvist, D. B. Suyatin, S. Suihkonen, E. I. Kauppinen, and M. Sopanen, *J. Vac. Sci. Technol. A* **35**, 060603 (2017).
- ³¹T. Ohba, W. B. Yang, S. Tan, K. J. Kanarik, and K. Nojiri, *Jpn. J. Appl. Phys., Part 1* **56**, 06HB06 (2017).
- ³²J. K. Hite, M. A. Mastro, and C. R. Eddy, *J. Cryst. Growth* **312**, 3143–3146 (2010).
- ³³J. W. Clancey, A. S. Cavanagh, R. S. Kukreja, A. Kongkanand, and S. M. George, *J. Vac. Sci. Technol. A* **33**, 01A130 (2015).
- ³⁴*HSC Chemistry*, HSC Chemistry 5.1, Outokumpu Research Oy (Pori, Finland).
- ³⁵V. M. Bermudez, *Appl. Surf. Sci.* **119**, 147–159 (1997).
- ³⁶M. Leszczynski, T. Suski, P. Perlin, H. Teisseyre, I. Grzegory, M. Bockowski, J. Jun, S. Porowski, and J. Major, *J. Phys. D: Appl. Phys.* **28**, A149–A153 (1995).
- ³⁷B. E. Deal and A. S. Grove, *J. Appl. Phys.* **36**, 3770–3778 (1965).
- ³⁸H. Z. Massoud, J. D. Plummer, and E. A. Irene, *J. Electrochem. Soc.* **132**, 2685–2693 (1985).